A phenomenological model of deformation twinning kinetics

A. Vinogradov

Department of Mechanical and Industrial Engineering, Norwegian University of Science and Technology – NTNU, Trondheim 7491, Norway

Abstract. Inspired by the classical Olson and Cohen model for martensitic phase transformations, a simple phenomenological model of the deformation twinning kinetics is proposed with account for twin-twin interactions. The model was validated for different materials using experimental data abundantly available in the literature for the evolution of the twin volume fraction with strain.

Keywords: mechanical twinning; phenomenological modelling; acoustic emission

1. Introduction and Motivation

With the advent of new structural materials whose microstructural evolution under load is mediated by mechanical twinning, understanding of the kinetics of this process becomes crucial [1, 2]. The role of twinning is central in the mechanical response of many contemporary materials such as low stacking-fault energy face-centred cubic (fcc) metals and alloys including copper-based alloys [3-5], high manganese Hadfield steels [6-9] and austenitic steels with the TWIP (TWinning Induced Plasticity) effect [10-13], hexagonal close-packed (HCP) titanium and its alloys [14], magnesium and its alloys [15], as well as modern high entropy alloys [16] and many nanostructured materials where the dislocation activity is inhibited by grain boundaries [17-19]. Plenty of investigations have been conducted on Mg and its alloys, which exhibit the strain hardening behaviour with remarkable features including a concave shape of the stress-strain curve and a pronounced asymmetry of the yield strength with respect to tension/compression caused by profuse

twinning [20-24]. While the dislocation slip-controlled plasticity is understood in minute details, the role of twinning and its strain/stress dependent kinetics in the strain hardening process has been rationalised to a much lesser extent. Since nearly all aspects of the stress-strain response of materials, which are prone to twinning, depend on the twin density, the constitutive description of the twin accumulation process is pivotal in virtually all models of the strain hardening behaviour of materials of this kind. For example, the twin volume fraction F evolving with strain is considered to limit the mean free path of dislocations, thus giving rise to the so-called dynamic Hall-Petch effect [11, 25].

For the variation of the twin volume fraction F with the total strain ε in high manganese TWIP steels, Bouaziz and Guelton [26] (see also [27-29]) suggested that the volume fraction of twins inside the grains which undergo deformation twinning can be derived using the first-order kinetics assumption similar to that made by Olson and Cohen [30] for the martensitic phase transformation. In that approach, F as a function of strain ε is governed by the following kinetic equation

$$dF\left(\varepsilon\right) = (1-F)m d\varepsilon \tag{1}$$

where F is the volume fraction of twins and $\left(1-F\right)$, therefore, refers to the fraction of the untwinned material where twins may form at a rate determined by the microstructurally sensitive factor *m* that depends on the stacking fault energy. After elementary integration (with the initial condition $F\left(0\right)=0$) the twin volume fraction is expressed as

$$F\left(\varepsilon\right) = 1-\exp\left(-m\varepsilon\right) \tag{2}$$

A non-zero initial twin volume fraction can be, of course, assumed as well [31]. Although this simple equation does reflect the trend of $F(\varepsilon)$ to saturation with growing strain, Fig.2a in a general manner, it does not capture the S-shaped twin accumulation behaviour reported frequently for different materials, cf. Fig.1. Besides, it contradicts the vast majority of acoustic emission (AE) observations carried out on materials with twinning-mediated plasticity [32-40]. Indeed, while the first strain derivative

$$F'\left(\varepsilon\right) = m\exp(-m\varepsilon) \tag{3}$$

predicts twinning activity with a highest magnitude at $\varepsilon = 0$, rapidly dropping off with strain, the twinning-induced AE often exhibits a pronounced bell-shaped peak at non-zero plastic strains as will be further discussed in what follows. (In Eq. (3) and below a prime refers to a derivative with respect to strain.)

In a more general, though heuristic, formulation used by Barnett et al. [41], the strain-dependent kinetics of the evolution of the twin volume fraction is represented by a characteristic S-shape dependence on the imposed strain as

$$F(\varepsilon) = F_S\left(1 - \exp\left[-4\left(\varepsilon / \varepsilon_e\right)^n\right]\right) \tag{4}$$

Here ε_e is the macroscopic strain at which the twinning reaction is 98% complete; the saturation twin volume fraction F_S is introduced in the last expression. A somewhat different form of the $F(\varepsilon)$ function was proposed by Bouaziz et al. [26, 28] (see also [11, 42]):

$$F(\varepsilon) = F_S\left(1 - \exp\left[-\beta\left(\varepsilon - \varepsilon_i\right)^n\right]\right)^{m^*} \tag{5}$$

where ε_i is a critical strain for the onset of nucleation of twins. According to the probabilistic model for twin nucleation proposed by Beyerlein and Tome [43], the F_S value is controlled by the initial density of grain boundary twin sources and, therefore, by the grain size. The parameters *n*, β, and *m** are adjustable quantities which need to be determined experimentally. Since it is practically impossible to interpret these fitting parameters from any microstructurally informed models, it is highly desirable to develop a facile, yet phenomenologically tractable, model capable of describing the main features of twin accumulation during plastic deformation. To that end, the time-proven Equation (1) can be modified to allow for a more general S-shape kinetics of twin accumulation without sacrificing its phenomenological transparency. We should note that this equation, by its nature, does not imply any twin-twin interactions, thus missing their crucial significance for the accumulation of deformation twins and for the overall strain hardening behaviour of materials whose deformation is governed by mechanical twinning [25, 44-46]. In this context, it is timely to recall that the statistical analysis of acoustic emission time series recorded from plastically deforming polycrystalline magnesium-based ZK60 alloy and single crystalline pure Mg revealed that mechanical twinning belongs to a class of non-Poisson processes with a relatively long memory of the past [47, 48] (the same conclusion applies to titanium and TWIP-steels). There is abundant evidence to support this premise. Multiple experimental and modelling efforts (e.g. [49-53]) devoted to assess the twin local stresses have demonstrated that the nucleation of the twin induces localised long-range stress fields which are much greater in magnitude than the average stresses caused by the external loading in the matrix. The twin

nucleated at the grain boundary propagates in the in-twin-plane directions, terminating finally at the opposite grain boundaries where the stress fields can be relaxed either by dislocation slip or by a new twin that can be nucleated at the twin tip in the same or neighbouring grain. In this "relay-like" behaviour, the parent twins follow a Poisson process while the descendants (child twins) are triggered in the close proximity to the parent twins giving rise to the observed memory of the past in AE times series [47, 48]. The results of direct video observations corroborate the proposed scenario as demonstrated in Fig.3 by a sequence of light microscopic images obtained during early stages of tensile straining of the as-cast alloy ZK60 (see [54] for experimental details). One can see, for example, that the twin generated in Fig.3b becomes a parent to the child twin subsequently generated in Fig.3c. The same can be seen in the pairs of snapshots shown in Fig.3 d-e, and Fig.3 c-f. These in situ observations are similar in sense to numerous microscopic observations ex situ, e.g. [50, 55-57]. The molecular dynamic simulations performed in [58] also validate this scenario on the microscale. An important corollary from these observations is that twin-twin interactions affecting the kinetics of twin nucleation must be taken into account if a predictive capability is to be attained in modelling the mechanical behaviour of materials with twinning-mediated plasticity.

2. Model

Thus, being inspired by the classical Olson and Cohen model and motivated by the self-evident need for a more generally applicable model of twin accumulation, we propose the following phenomenological microstructurally-based approach accounting for the probability of twin nucleation in the untwinned volume and for the probability of the self-exciting twin nucleation. Starting from the premises stated in the preceding section and assuming that the twinning kinetics is nucleation-controlled, rather than growth controlled, the self-influencing interaction can be incorporated into the Olson-Cohen kinetic equation through the additional term associated with the conditional twin nucleation probability around a parent twin. The additional term is proportional to the volume fractions of the twinned and untwinned regions, and, thus, the modified kinetic equation can be written as

$$dF\left(\varepsilon\right)=(1-F)md\varepsilon+(1-F)Fld\varepsilon \tag{6}$$

where *l* is a rate-controlling parameter for twin production due to twin-twin interactions. The general solution of this ordinary differential equation satisfying the zero initial condition is

$$F\left(\varepsilon\right)=F_S\frac{m\left[\exp\left(\varepsilon\left(m+l\right)\right)-1\right]}{1+m\exp\left(\varepsilon\left(m+l\right)\right)} \tag{7}$$

which reduces to the familiar Olson- Cohen form, Eq.(2), at $l \ll m$ and predicts an S-shaped twinning kinetic otherwise, as illustrated schematically in Fig.2. The saturation twin volume fraction F_S is introduced as a factor in the above equation, similarly to that in Eq.(5).

The first strain derivative of this function, F', reflecting the activity of twin sources is given by

$$F'(\varepsilon) = F_S \frac{m(m+l)^2 \exp\left[\varepsilon(m+l)\right]}{\left(1+m\exp\left[\varepsilon(m+l)\right]\right)^2} \tag{8}$$

It behaves either as is expected from the Olson-Cohen equation (as shown by a dashed line in Fig.2d) at $l \ll m$, or exhibits a pronounced skewed peak at a strain ε_p satisfying the maximum condition $F''(\varepsilon_p) = 0$ at

$$\varepsilon_p = \frac{\ln(l/m)}{m+l} \tag{9}$$

The maximum value of the twin accumulation rate, $F'(\varepsilon_p)$, is determined by a combination of two parameters entering the model as

$$F'(\varepsilon_p) = \frac{(l+m)^2}{4l} \tag{10}$$

The model predicts plausibly that the twin accumulation rate tends to zero as deformation proceeds and the twin volume fraction saturates. The intercept of the F' curve with the strain axis at zero strain (or, more precisely, at a small strain corresponding to the onset of twinning) equals *m*.

3. Model Validation and Discussion

A common way of validating any phenomenological model is to compare its predictions with experimental data. The present model was verified in two independent ways: by fitting Eq.(7) to the available experimental data for the twin volume fraction measured as a function of plastic strain in different materials, and by comparing the twinning accumulation and the respective rate with the AE results.

The experimental data presented in Fig.1 reported for different materials for high manganese austenitic TWIP steels ([59, 60] (a), Titanium [61] and Zirconium [62] (b), Mg and its alloys [63-66] (c), and a low stacking fault Cu-33Ni alloy [67] and high entropy CoCrFeMnNi alloy [68, 69] (d) – see the cited papers for experimental details) are matched by the proposed model, Eq.(7), very well. This is shown by the red lines in Fig.1 obtained using nonlinear regression by the Levenberg-Marquardt algorithm. Many other data for similar materials, e.g. [70-77], which are not shown here, have also been tested against the proposed model. Without fail, the model demonstrates excellent agreement with the experimental results for a wide range of structural materials experiencing profuse twinning under load.

Since the model represents the twin nucleation process, it can be further verified by means of the acoustic emission technique, which is known to be particularly sensitive to twin nucleation events [65, 78, 79], and

which is frequently used to assess the accumulation of mechanically induced twins or martensite lamella, cf. [37]. The experimental AE data, which have been previously reported for the same group of materials deforming in tension with the considerable contribution from the twinning mechanism are rearranged and plotted in Fig.4 to allow for the comparison of the AE behaviour with the model predictions. The experimental details and the features of the microstructure evolution of the materials studied can be found in the original publications: [37] for the high-alloyed Fe-16Cr-6Mn-9Ni (in wt.%) cast austenitic stainless steel, [65] for the as-cast pure Mg polycrystal, [36] for the Mg-Zn-Zr alloy ZK60, and [5] for the low stacking fault Cu-9Ge (in at.%) alloy. It is essential to notice, that in all works cited, the broadband AE measurements were followed by the signal classification procedure capable of distinguishing signals associated with twinning events from the overall AE flow influenced by dislocation slip, (cf. also [80] for the clustering methods used). Thus, the results shown in Fig.4 refer to the AE due to contribution from twinning only and can be used for the comparison with the model. The model predicts a skewed bell-shaped curve for the rate of the twinning accumulation, Fig.2d. The position and the height of the peak depend on the *m* and *l* values, which are material specific. The average AE power P_{AE} reflecting the rate of twin accumulation does exhibit the anticipated response in congruence with Eq.(8), Fig.4. It is worth noting that the model also predicts the non-zero offset of the twin accumulation rate curve as deformation twinning sets in, which is determined solely by the *m*-value of the Olson-Cohen model, Eq.(2), Fig.2b. This is a plausible result since the twin-twin interactions are deemed negligible at the small strains. The offset is clearly discernible in the experimental data as shown by horizontal dashed lines intersecting the P_{AE} axis in Fig.4a, b. The Cu-9Ge alloy exhibits a very sharp twinning-related AE peak at the onset of loading where the stress-strain curve exhibits the characteristic plateau-like feature. The evolution of twins in this material is nicely captured by the single-variable Olson-Cohen model, since *l* identified through fitting the model to experimental data turns out to be much smaller than *m*, suggesting that mutual twinning interactions are negligible in this material. Therefore, a sharp AE peak followed by a rapid decay in P_{AE} is observed in this material at the early loading stage. The cumulative AE power $\Sigma P_{AE}(\varepsilon)$ obtained as the integral of $P_{AE}(\varepsilon)$ and normalised to unity for convenience, reflects the evolution of the twin density with strain, albeit in relative terms. The smooth integral $\Sigma P_{AE}(\varepsilon)$ curve (shown in green) has the characteristic S-shape, which can be nearly perfectly approximated by the model, Eq.(7), as shown by the red lines.

The present nucleation-based model can be fine-tuned to situations where the twin growth is significant. While twin thickening is not an important consideration in many fcc metals and alloys including TWIP steels, it can be essential in hcp materials such as magnesium, titanium and their alloys. In the first order approximation, the twin growth can be implicitly accounted for, on average, through the scaling factor F_S

Explicit accounting for the twin thickening would require a separate kinetic equation for the twin

thickness as a function of strain, strain rate and temperature. Not only the explicit form of such an equation is known to date, but this would complicate the analysis substantially with additional phenomenological parameters and interactions involved. Again, our point is that a simple transparent model with high predictive capacity and few physically motivated variables does have its merits and advantages over more sophisticated ones or over purely empiric curve-fitting approaches representing the $F(\varepsilon)$ behaviour.

The values of the rate-controlling parameters *m* and *l* are microstructure sensitive. They cannot be determined within the proposed phenomenological formulation, and their magnitude needs to be calculated in terms of microstructure-based models accounting for the specifics of the deformation twinning process in different materials. While this is a scope of future work, the numerical values of these parameters can readily be determined either from the nonlinear curve fit of the $F(\varepsilon)$ data, like that shown in Fig.1. The AE data of the kind presented in Fig.4 can be used for that purpose too. By using the initial offset of the AE power curve and the height and position of the AE peak with respect to strain (Eqs. (9) and (10), respectively), one can determine both *m* and *l* values. The kinetics of twin accumulation can then be unravelled based on Eq.(7), at least semi-quantitatively. To enable a quantitative description of the entire $F(\varepsilon)$ curve, calibration of the AE data is required, which can be done by introducing a scaling factor to Eq.(7). For this calibration, at least one datapoint for the twin volume fraction along the strain path needs to be known from independent measurements. The proposed model, which has been validated by using data from two independent experimental techniques, provides a reliable and practicable platform for such procedures.

4. Conclusion

In conclusion, the main thrust of the present work was to propose a general phenomenological model explicitly relating the twin volume fraction to plastic strain with account of twin-twin interactions. Based on the first-order kinetics approach using only physically motivated variables, the proposed model is capable of accurately predicting twin accumulation behaviour in different materials with twinning-mediated plasticity. These predictions were verified by two independent types of experiments, which testifies to its credibility. The model also provides a general platform for accounting for the commonly observed features of the acoustic emission behaviour. Besides, the acoustic emission was shown to be a simple, yet viable, tool to retrieve the model parameters.

Acknowledgements. The author is thankful to Professor Yuri Estrin for his stimulating interest and numerous fruitful discussions.

This research did not receive any specific grant from funding agencies in the public, commercial, or not-for-profit sectors.

Data availability. The data that support the findings of this study are available from the author upon reasonable request.

References

[1] L. Lu, Y. Shen, X. Chen, L. Qian, K. Lu, Science, 304 (2004) 422-426.
[2] X.L. Wu, Y.T. Zhu, Physical Review Letters, 101 (2008) 025503.
[3] M. Hatherly, A.S. Malin, Metals Technology, 6 (1979) 308-319.
[4] R. Liu, Z.J. Zhang, L.L. Li, X.H. An, Z.F. Zhang, Scientific Reports, 5 (2015) 9550.
[5] A. Vinogradov, D.L. Merson, V. Patlan, S. Hashimoto, Materials Science and Engineering A, 341 (2003) 57-73.
[6] I. Karaman, H. Sehitoglu, A.J. Beaudoin, Y.I. Chumlyakov, H.J. Maier, C.N. Tomé, Acta Materialia, 48 (2000) 2031-2047.
[7] I. Karaman, H. Sehitoglu, Y. Chumlyakov, H. Maier, JOM Journal of the Minerals, Metals and Materials Society, 54 (2002) 31-37.
[8] I. Karaman, H. Sehitoglu, K. Gall, Y.I. Chumlyakov, H.J. Maier, Acta Materialia, 48 (2000) 1345-1359.
[9] M. Lindroos, A. Laukkanen, G. Cailletaud, V.-T. Kuokkala, International Journal of Solids and Structures, 125 (2017) 68-76.
[10] G. Frommeyer, U. Brux, P. Neumann, ISIJ International, 43 (2003) 438-446.
[11] B.C. De Cooman, Y. Estrin, S.K. Kim, Acta Materialia, 142 (2018) 283-362.
[12] I. Gutierrez-Urrutia, D. Raabe, Acta Materialia, 59 (2011) 6449-6462.
[13] A. Weidner, Deformation Processes in TRIP/TWIP Steels, Springer, Cham, Switzerland 2020.
[14] A.A. Salem, S.R. Kalidindi, R.D. Doherty, Acta Materialia, 51 (2003) 4225-4237.
[15] C. Bettles, M. Barnett, Advances in wrought magnesium alloys: Fundamentals of processing, properties and applications, Woodhead Publishing Ltd., Philadelphia, USA, 2012.
[16] Y. Wang, B. Liu, K. Yan, M. Wang, S. Kabra, Y.-L. Chiu, D. Dye, P.D. Lee, Y. Liu, B. Cai, Acta Materialia, 154 (2018) 79-89.
[17] K. Lu, L. Lu, S. Suresh, Science, 324 (2009) 349-352.
[18] Y. Li, Y.H. Zhao, W. Liu, C. Xu, Z. Horita, X.Z. Liao, Y.T. Zhu, T.G. Langdon, E.J. Lavernia, Materials Science and Engineering: A, 527 (2010) 3942-3948.
[19] Y.T. Zhu, X.Z. Liao, X.L. Wu, Progress in Materials Science, 57 (2012) 1-62.
[20] M.R. Barnett, Materials Science and Engineering A, 464 (2007) 1-7.
[21] M.R. Barnett, Materials Science and Engineering A, 464 (2007) 8-16.
[22] S.R. Agnew, Deformation mechanisms of magnesium alloys, in: C. Bettles, M. Barnett (Eds.) Advances in Wrought Magnesium Alloys: Fundamentals of Processing, Properties and Applications, 2012, pp. 63-104.
[23] K. Máthis, F. Chmelík, M. Janeček, B. Hadzima, Z. Trojanová, P. Lukáč, Acta Materialia, 54 (2006) 5361-5366.
[24] B.C. Suh, M.S. Shim, K.S. Shin, N.J. Kim, Scripta Materialia, 84-85 (2014) 1-6.
[25] M. Bönisch, Y. Wu, H. Sehitoglu, Acta Materialia, 153 (2018) 391-403.
[26] O. Bouaziz, N. Guelton, Materials Science and Engineering: A, 319–321 (2001) 246-249.
[27] S. Allain, J.P. Chateau, O. Bouaziz, Materials Science and Engineering: A, 387–389 (2004) 143-147.
[28] O. Bouaziz, S. Allain, C. Scott, Scripta Materialia, 58 (2008) 484-487.
[29] O. Bouaziz, Scripta Materialia, 66 (2012) 982-985.
[30] G.B. Olson, M. Cohen, Metallurgical Transactions A, 6 (1975) 791-795.
[31] D.-H. Ahn, H.S. Kim, Y. Estrin, Scripta Materialia, 67 (2012) 121-124.
[32] J. Bohlen, P. Dobroň, J. Swiostek, D. Letzig, F. Chmelík, P. Lukáč, K.U. Kainer, Materials Science and Engineering: A, 462 (2007) 302-306.
[33] O. Muransky, M.R. Barnett, D.G. Carr, S.C. Vogel, E.C. Oliver, Acta Materialia, 58 (2010) 1503-1517.
[34] K. Máthis, J. Čapek, Z. Zdražilová, Z. Trojanová, Materials Science and Engineering A, 528 (2011) 5904-5907.
[35] Y. Li, M. Enoki, Materials Science and Engineering: A, 536 (2012) 8-13.
[36] A. Vinogradov, D. Orlov, A. Danyuk, Y. Estrin, Acta Materialia, 61 (2013) 2044-2056.
[37] A. Vinogradov, A. Lazarev, M. Linderov, A. Weidner, H. Biermann, Acta Materialia, 61 (2013) 2434-2449.
[38] M. Linderov, C. Segel, A. Weidner, H. Biermann, A. Vinogradov, Materials Science and Engineering A, 597 (2014) 183-193.
[39] D. Drozdenko, J. Bohlen, S. Yi, P. Minárik, F. Chmelík, P. Dobroň, Acta Materialia, 110 (2016) 103-113.
[40] D. Drozdenko, J. Čapek, B. Clausen, A. Vinogradov, K. Máthis, Journal of Alloys and Compounds, 786 (2019) 779-790.
[41] M.R. Barnett, Materials Science Forum, 2005, pp. 1079-1084.
[42] G.-H. Zhao, X. Xu, D. Dye, P.E.J. Rivera-Díaz-del-Castillo, Acta Materialia, 183 (2020) 155-164.

[43] I.J. Beyerlein, C.N. Tomé, Proceedings of the Royal Society of London A: Mathematical, Physical and Engineering Sciences, 466 (2010) 2517-2544.
[44] Q. Yu, J. Wang, Y. Jiang, R.J. McCabe, N. Li, C.N. Tomé, Acta Materialia, 77 (2014) 28-42.
[45] P. Müllner, International Journal of Materials Research, 97 (2006) 205-216.
[46] I. Basu, T. Al-Samman, Frontiers in Materials, 6 (2019).
[47] A. Vinogradov, E. Agletdinov, D. Merson, Scientific Reports, 9 (2019) 5748.
[48] E. Agletdinov, D. Drozdenko, P. Harcuba, P. Dobroň, D. Merson, A. Vinogradov, Materials Science and Engineering: A, 777 (2020) 139091.
[49] L. Balogh, S.R. Niezgoda, A.K. Kanjarla, D.W. Brown, B. Clausen, W. Liu, C.N. Tomé, Acta Materialia, 61 (2013) 3612-3620.
[50] Y. Guo, H. Abdolvand, T.B. Britton, A.J. Wilkinson, Acta Materialia, 126 (2017) 221-235.
[51] H. Abdolvand, O. Sedaghat, Y. Guo, Materialia, 2 (2018) 58-62.
[52] H. Abdolvand, A.J. Wilkinson, Acta Materialia, 105 (2016) 219-231.
[53] M. Arul Kumar, B. Clausen, L. Capolungo, R.J. McCabe, W. Liu, J.Z. Tischler, C.N. Tomé, Nature Communications, 9 (2018) 4761.
[54] M. Seleznev, A. Vinogradov, Review of Scientific Instruments, 85 (2014) 076103.
[55] S. Mahajan, G.Y. Chin, 21 (1973) 173-179.
[56] A. Khosravani, D.T. Fullwood, B.L. Adams, T.M. Rampton, M.P. Miles, R.K. Mishra, Acta Materialia, 100 (2015) 202-214.
[57] M. Arul Kumar, L. Capolungo, R.J. McCabe, C.N. Tomé, Scientific Reports, 9 (2019) 3846.
[58] Z. Li, B. Xu, W. Liu, Computational Materials Science, 154 (2018) 147-151.
[59] K. Renard, P.J. Jacques, Materials Science and Engineering: A, 542 (2012) 8-14.
[60] D. Barbier, N. Gey, N. Bozzolo, S. Allain, M. Humbert, Journal of Microscopy, 235 (2009) 67-78.
[61] A.A. Salem, S.R. Kalidindi, S.L. Semiatin, Acta Materialia, 53 (2005) 3495-3502.
[62] R.J. McCabe, G. Proust, E.K. Cerreta, A. Misra, International Journal of Plasticity, 25 (2009) 454-472.
[63] B. Clausen, C.N. Tome, D.W. Brown, S.R. Agnew, Acta Materialia, 56 (2008) 2456-2468.
[64] J. Čapek, J. Stráská, B. Clausen, K. Máthis, Acta Physica Polonica A, 128 (2015) 762-764.
[65] K. Máthis, G. Csiszár, J. Čapek, J. Gubicza, B. Clausen, P. Lukáš, A. Vinogradov, S.R. Agnew, International Journal of Plasticity, 72 (2015) 127-150.
[66] K. Máthis, J. Čapek, B. Clausen, T. Krajňák, D. Nagarajan, Journal of Alloys and Compounds, 642 (2015) 185-191.
[67] L. Rémy, Acta Metallurgica, 25 (1977) 711-714.
[68] J. Moon, S.I. Hong, J.W. Bae, M.J. Jang, D. Yim, H.S. Kim, Materials Research Letters, 5 (2017) 472-477.
[69] T.K. Liu, Z. Wu, A.D. Stoica, Q. Xie, W. Wu, Y.F. Gao, H. Bei, K. An, Materials & Design, 131 (2017) 419-427.
[70] D.R. Steinmetz, T. Jäpel, B. Wietbrock, P. Eisenlohr, I. Gutierrez-Urrutia, A. Saeed-Akbari, T. Hickel, F. Roters, D. Raabe, Acta Materialia, 61 (2013) 494-510.
[71] A. Ghaderi, M.R. Barnett, Acta Materialia, 59 (2011) 7824-7839.
[72] J. Singh, S. Mahesh, G. Kumar, P. Pant, D. Srivastava, G.K. Dey, N. Saibaba, I. Samajdar, Metall and Mat Trans A, 46 (2015) 5058-5071.
[73] P. Rangaswamy, M.A.M. Bourke, D.W. Brown, G.C. Kaschner, R.B. Rogge, M.G. Stout, C.N. Tomé, Metall and Mat Trans A, 33 (2002) 757-763.
[74] A. Soulami, K.S. Choi, Y.F. Shen, W.N. Liu, X. Sun, M.A. Khaleel, Materials Science and Engineering: A, 528 (2011) 1402-1408.
[75] E.I. Galindo-Nava, Materials & Design, 83 (2015) 327-343.
[76] H. Pan, F. Wang, L. Jin, M. Feng, J. Dong, Journal of Materials Science & Technology, 32 (2016) 1282-1288.
[77] S.R. Agnew, C.A. Calhoun, J.J. Bhattacharyya, in: N.R. Neelameggham, A. Singh, K. Solanki, M.V. Manuel (Eds.), Minerals, Metals and Materials Society, 2016, pp. 189-194.
[78] R.L. Bell, R.W. Cahn, Proceedings of the Royal Society of London A: Mathematical, Physical and Engineering Sciences, 239 (1957) 494-521.
[79] A. Vinogradov, E. Vasilev, M. Seleznev, K. Máthis, D. Orlov, D. Merson, Materials Letters, 183 (2016) 417-419.
[80] E. Pomponi, A. Vinogradov, Mech. Syst. Signal Proc., 40 (2013) 791-804.

Figures.

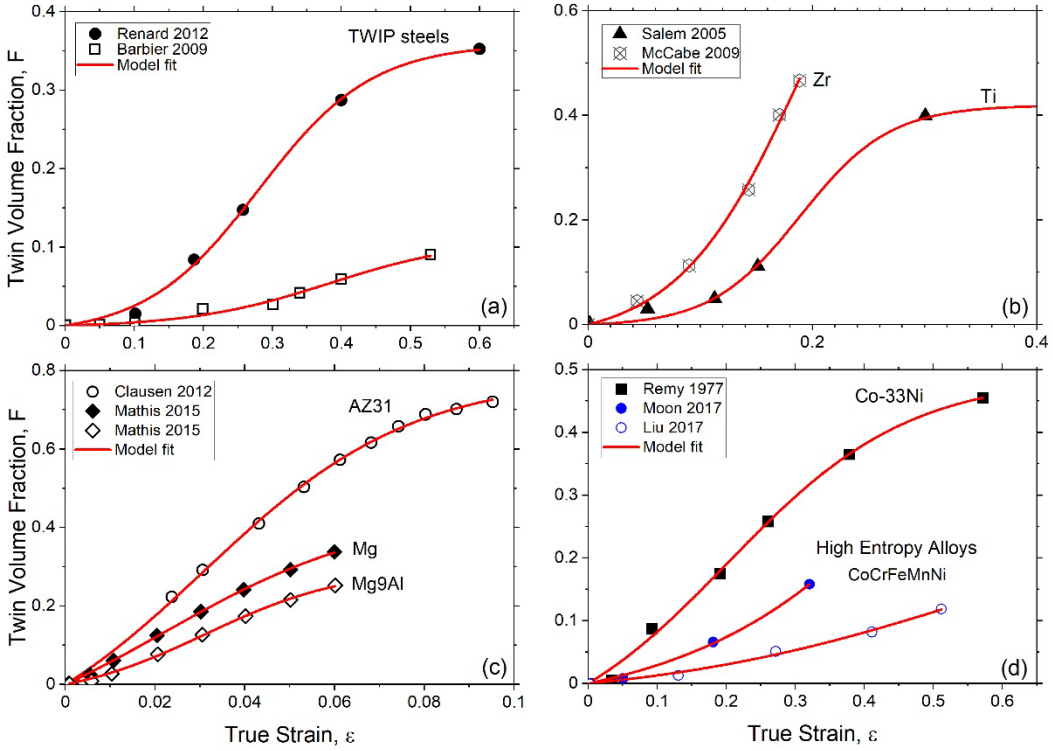

Figure 1. Experimental data for the twin volume fraction as a function of strain for different groups of materials: (a) fcc TWIP steels (b) hcp Zr and Ti (c) hcp Mg and its alloys and (d) low stacking fault fcc Cu-alloys and high entropy alloys. Model predictions are shown by solid lines.

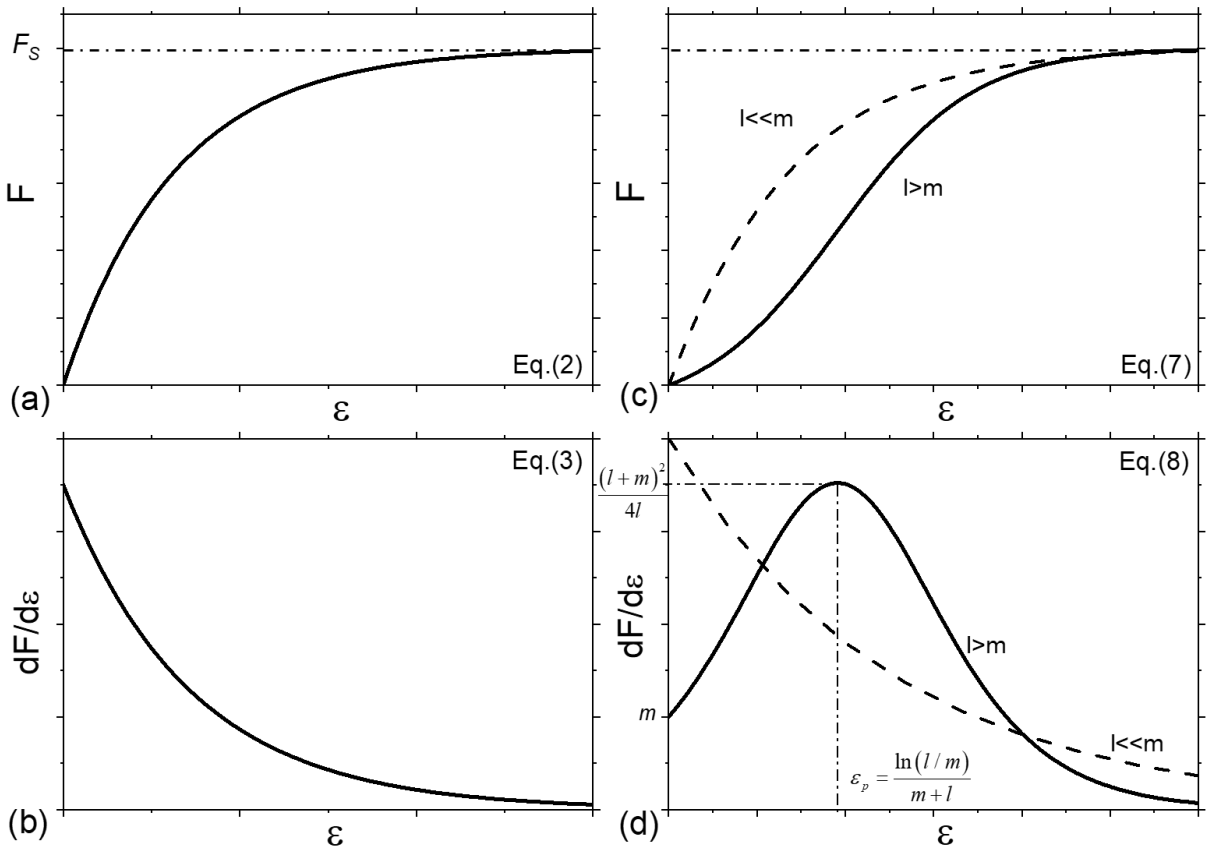

Figure 2. Schematic illustration showing the behaviour of the twin volume fraction *F* represented by the Olson-Cohen model according to Eq.(1) (a) and the corresponding twin accumulation rate $dF/d\varepsilon$ (b). The behaviour of the same quantities following the proposed model is shown in (c) and (d), respectively, for different combinations of entering parameters *m* and *l*.

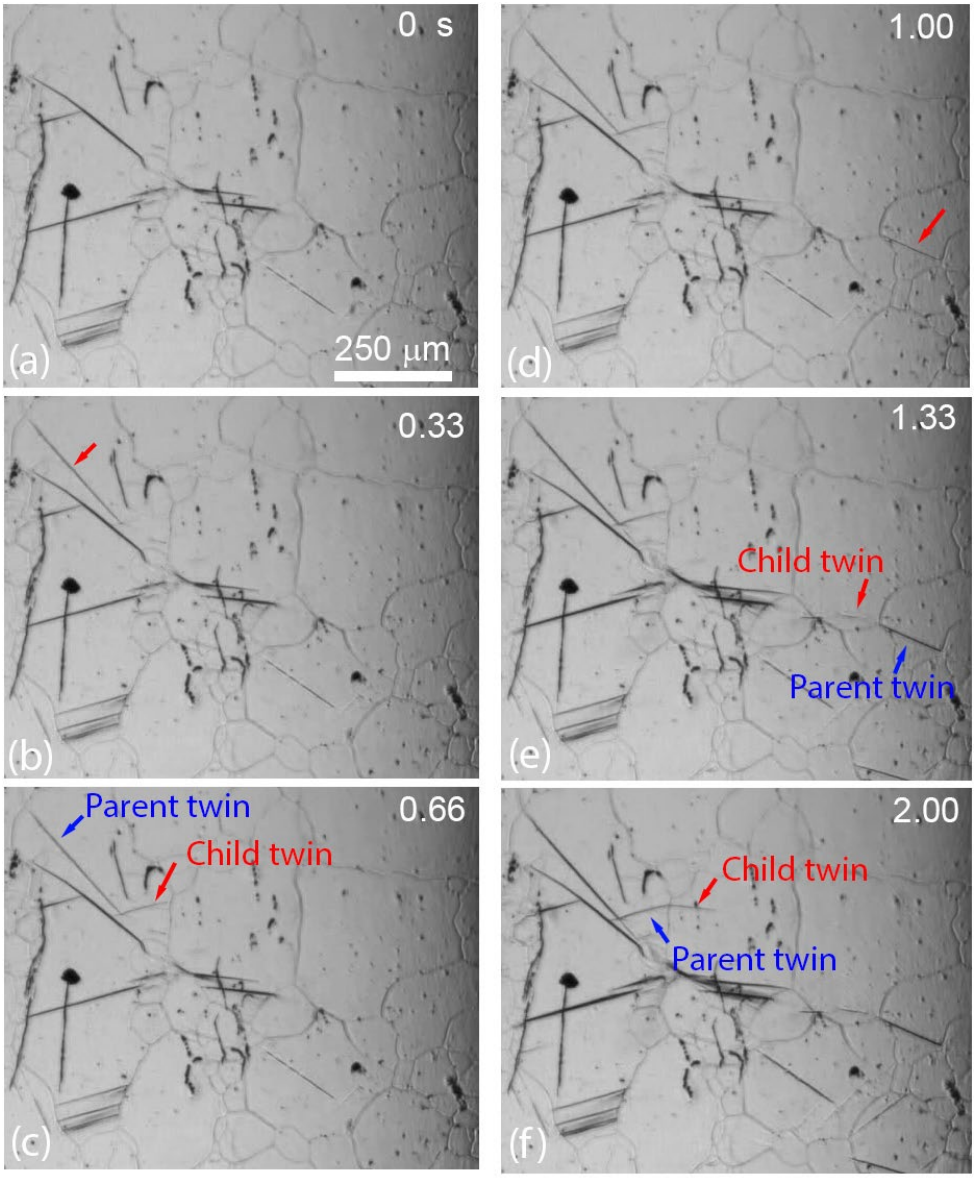

Figure 3. A sequence of light microscopic images obtained during early stages of tensile straining of the as-cast alloy ZK60. Time marks are shown in the upper right corner of each image. Freshly nucleated twins are indicated by red arrows; these twins can become parents for next generations of twins emerging in the close proximity to parents.

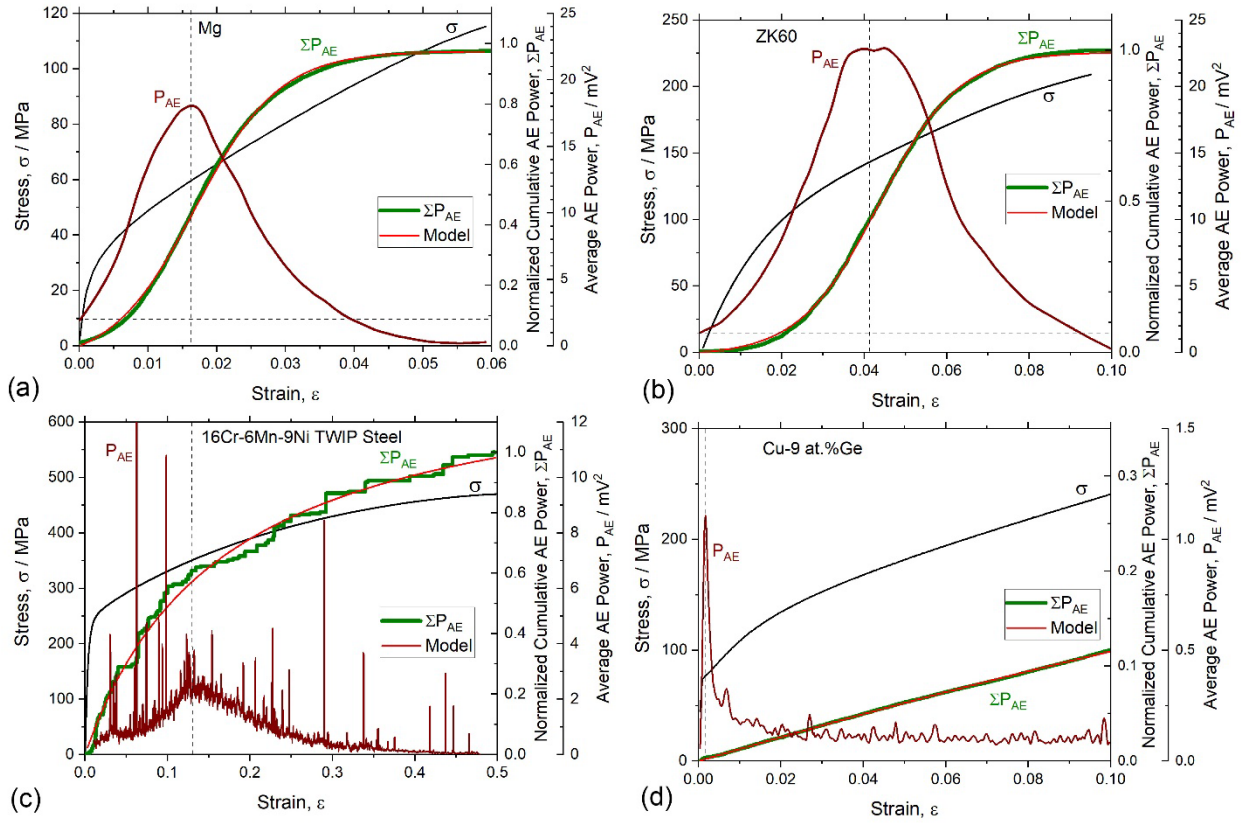

Figure 4. Verification of the proposed phenomenological model based on a comparison with the experimental acoustic emission data used to assess the evolution of the twin volume fraction in different materials. The twinning accumulation is represented by the cumulative AE power ΣP_{AE}, while the rate of twinning is supposed to be proportional to the average AE power P_{AE} (referred to 1 Ohm nominal impedance).